RESIDUAL INTERFERENCE AND WIND TUNNEL WALL ADAPTATION

Miroslav Mokry

National Aeronautical Establishment
National Research Council of Canada, Ottawa

I. Introduction

Measured flow variables near the test section boundaries, used to guide adjustments of the walls in adaptive wind tunnels, can also be used to quantify the residual interference. Because of a finite number of wall control devices (jacks, plenum compartments), the finite test section length, and the approximation character of adaptation algorithms, the unconfined flow conditions are not expected to be precisely attained even in the 'fully' adapted stage [1],[2].

The procedures for the evaluation of residual wall interference are essentially the same as those used for assessing the corrections in conventional, non-adaptive wind tunnels. Depending upon the number of flow variables utilized, we speak of *one-* or *two-variable* methods [3]; in two dimensions also of *Schwarz-* or *Cauchy-type* methods [4].

The one-variable methods use the measured static pressure distribution at the test section boundary and supplement it with the far field representation of the model, estimated from its geometry and measured forces.

The two-variable methods use measurements of static pressure and normal velocity at the test section boundary, but do not require any model representation. This is clearly of an advantage for adaptive wall test sections, which are often relatively small with respect to the test model, and for the variety of complex flows commonly encountered in wind tunnel testing. For test sections with flexible walls the normal component of velocity is given by the shape of the wall, adjusted for the displacement effect of its boundary layer. For ventilated test section walls it has to be measured by the Calspan Pipes, Laser Doppler Velocimetry, or other appropriate techniques.

The *interface discontinuity method*, also described, is a 'genuine' residual interference assessment technique. It is specific to adaptive wall wind tunnels, where the computation results for the fictitious flow in the exterior of the test section are provided.

II. Linear Flow Analysis

Since the adaptive walls introduce only minor disturbances to the unconfined far field of the test model, the linearization of the potential equation near the walls is applicable as long as the flow remains subcritical there.

The governing equation for the disturbance velocity potential is

$$\beta^2 \frac{\partial^2 \phi}{\partial x^2} + \frac{\partial^2 \phi}{\partial y^2} + \frac{\partial^2 \phi}{\partial z^2} = 0, \tag{1}$$

where $\beta = \sqrt{1 - M_\infty^2}$, and $M_\infty < 1$ is the stream Mach number.

The scaling of the streamwise coordinate,

$$x' = \frac{x}{\beta}, \tag{2}$$

reduces Eq.(1) to Laplace's equation, $\nabla^2 \phi = 0$.

The linear flow region where ϕ satisfies Eq.(1) is shown schematically in Fig.1a. It excludes the volume occupied by the test model, its viscous and transonic flow regions, and the wind tunnel exterior, where no real flow exists. The outer bounding surface, enclosing the test model, is expected to lie entirely within the linear flow region, off the viscous or nonisentropic flow at the walls.

Using the principle of linear superposition, the disturbance velocity potential is split as [5]

$$\phi = \phi_m + \phi_w, \tag{3}$$

where ϕ_m is that due to the model in free air and ϕ_w is that due to wall interference.

The model potential, ϕ_m, satisfies Eq.(1) in the infinite space outside the model and the adjacent nonlinear flow regions, Fig.1b.

The wall interference potential, ϕ_w, is assumed to satisfy Eq.(1) in the entire test section interior, including the model and its nonlinear flow regions, as indicated in Fig.1c.

This assignment of the singular and nonsingular parts as the effects of the model and the walls respectively is consistent with the concept of Green's function for the Laplace operator. Accordingly, it is rigorous for an infinitesimal model, but only approximate for a finite-size model.

The derivatives of ϕ_w are interpreted as disturbances to stream velocity components. They are usually evaluated at the model reference station or as averages over the model and interpreted as *global corrections* to stream Mach number [6]

$$\Delta M_\infty = (1 + \frac{\gamma - 1}{2} M_\infty^2) M_\infty \frac{\partial \phi_w}{\partial x}, \tag{4}$$

and to flow angles (in radians)

$$\Delta \alpha_y = \frac{\partial \phi_w}{\partial y} \quad \text{and} \quad \Delta \alpha_z = \frac{\partial \phi_w}{\partial z}. \tag{5}$$

From the spatial variations of these corrections over the model additional streamline curvature and buoyancy effects on model force data can be determined.

In connection with adaptive wall wind tunnels, another type of the disturbance velocity potential is helpful: that corresponding to the 'fictitious' flow outside the wind tunnel.

The potential, denoted here by the symbol $\tilde{\phi}$, satisfies Eq.(1) in the exterior of the outer bounding surface, Fig.1d. The surface, separating the real wind tunnel flow and the computed exterior flow is also termed the *interface*. The aim of adaptation is to adjust the walls so that ϕ and $\tilde{\phi}$ constitute a single potential ϕ_m, continuous at the interface. There is a direct relationship between ϕ_w and the difference $\phi - \tilde{\phi}$ at the interface.

A. One-Variable Method

The method, due to *Capelier, Chevallier and Bouniol* [7], is the most popular technique for the assessment of subsonic wall interference in wind tunnels with perforated walls. It retains the essential features of the classical wall interference approach [5], but replaces the idealized wind tunnel boundary conditions by

$$\frac{\partial \phi}{\partial x} = -\frac{1}{2} C_p, \tag{6}$$

where C_p is the measured boundary pressure coefficient. The control surface along which the pressure is measured should be some distance away from the wall, where the disturbances of individual holes (perforations) are smeared out. The application of the method to test sections with slotted walls is more problematic as the flow becomes homogeneous at rather large distances from the walls, and the pressures measured directly on slat surfaces do not necessarily represent the averaged values.

The axial component of wall interference velocity,

$$u_w = \frac{\partial \phi_w}{\partial x}, \tag{7}$$

satisfying inside the test section

$$\beta^2 \frac{\partial^2 u_w}{\partial x^2} + \frac{\partial^2 u_w}{\partial y^2} + \frac{\partial^2 u_w}{\partial z^2} = 0, \tag{8}$$

is obtained from its boundary values

$$u_w = -\frac{1}{2} C_p - \frac{\partial \phi_m}{\partial x} \tag{9}$$

as a solution of the interior Dirichlet problem. The transverse velocity components,

$$v_w = \frac{\partial \phi_w}{\partial y} \qquad \text{and} \qquad w_w = \frac{\partial \phi_w}{\partial z}, \tag{10}$$

can be obtained from u_w by integrating the irrotational-flow conditions

$$\frac{\partial v_w}{\partial x} = \frac{\partial u_w}{\partial y} \qquad \text{and} \qquad \frac{\partial w_w}{\partial x} = \frac{\partial u_w}{\partial z} \tag{11}$$

along a path from the upstream end of the test section.

The Dirichlet problem for Laplace's equation is one of the best explored problems in mathematical physics and there are a large number of methods available to solve it numerically. A natural approach is to solve the problem in terms of the double layer potential [8], leading to a doublet panel method [9]. For simpler geometries, closed form solutions are obtainable using integral transforms [7] or the Fourier method [10]-[12].

The complex-variable treatment [7] of the two-dimensional problem leads, as pointed out in Ref.[4], to the Schwarz problem, consisting of determining an analytic function inside a domain from its defined real part on the boundary. Theory [13] shows that the integration of Cauchy-Riemann equations (irrotational-flow conditions) introduces an unknown imaginary constant, which needs to be specified in order to make the solution unique (specification of the upstream flow angle).

The accuracy of the one-variable method depends greatly on the accuracy with which the free air potential ϕ_m can be predicted on the control surfaces [14],[15]. Since the far field of ϕ_m is normally evaluated using the measured model loading, subject to wall interference, the prediction tends to be more exact near a fully adapted stage. However, when compared to the relative size of the model, the adaptive test sections are usually much narrower than the conventional ones, so that the representation of flow near the walls in terms of the model far field may not be satisfactory.

Another source of inaccuracy is the finite length of the test section and sparseness of the experimental pressure data. The boundary values of u_w have to be interpolated or extrapolated over a complete boundary (closed or infinite), in order to make the Dirichlet problem soluble. The adaptive test sections, which are typically longer than the conventional ones, will have a slight advantage in this regard.

The method can be used to monitor the reduction of wall interference corrections in the course of adaptation, but can also be incorporated into the adaptation algorithm [16]. Interference-free (unconfined) flow will be characterized by the vanishing boundary values of u_w:

$$u_w \equiv 0 \quad \text{on} \quad S. \tag{12}$$

Compensation for errors of reference velocity or pressure [7], also called the *autocorrective property* [15] or *autoconvergence* [17], is an important feature of the method. It applies within the limits of linearization and may be stated as follows: if the error of the (upstream) reference velocity U_∞ is δU_∞, then the perturbation velocities $U - U_\infty$ on the boundary will be offset by $-\delta U_\infty$. The ensuing incremental correction, being of equal magnitude but opposite sign to the reference velocity error, will restore U_∞ as the reference velocity.

For the one-variable method, working with measured boundary pressures p, the autocorrective property can easily be verified by introducing the pressure coefficient

$$C_p = \frac{p - p_\infty}{\frac{1}{2}\rho_\infty U_\infty^2},$$

and its error [6]

$$\delta C_p = \frac{p - (p_\infty + \delta p_\infty)}{\frac{1}{2}\rho_\infty U_\infty^2 + \delta\left(\frac{1}{2}\rho_\infty U_\infty^2\right)} - C_p$$
$$\simeq \left[2 - (2 - M_\infty^2)C_p\right]\frac{\delta U_\infty}{U_\infty}$$
$$\simeq 2\frac{\delta U_\infty}{U_\infty} \qquad \text{if} \quad C_p \simeq 0.$$

From Eq.(9), considering $\partial\phi_m/\partial x$ invariant, the boundary value of u_w is found to have a constant increment

$$\delta u_w = -\frac{1}{2}\delta C_p \simeq -\frac{\delta U_\infty}{U_\infty}, \tag{13}$$

which is equal and opposite to the relative error of reference velocity. This incremental correction also applies also interior points since

$$\delta u_w(x, y, z) = -\frac{\delta U_\infty}{U_\infty} = \text{constant}$$

is a solution of Eq.(8) satisfying the boundary condition (13). There are no other possibilities, as the solution to a Dirichlet problem is unique.

Besides compensating for genuine reference velocity errors, the autocorrective principle also establishes the correspondence between U_∞ based on plenum pressure and actual stream velocity in ventilated test sections.

B. Two-Variable Method

Measurement of the static pressure and normal velocity distributions along the control surface opens the possibility of evaluating subsonic wall interference bypassing the model representation. The two-variable method is most easily applied to solid wall test sections where the walls can serve as control surfaces.

Independent formulations of this concept using Green's theorem are due to *Ashill* and *Weeks* [18] and Cauchy's integral formula (in 2D) due to *J. Smith* [4].

To describe the method, we introduce the position vectors of an interior point and a boundary point,

$$\mathbf{r}_0 = (x_0', y_0, z_0) \qquad \text{and} \qquad \mathbf{r} = (x', y, z), \tag{14}$$

and denote by

$$G(\mathbf{r}_0, \mathbf{r}) = -\frac{1}{4\pi|\mathbf{r}_0 - \mathbf{r}|} \tag{15}$$

the fundamental solution (unit-strength source) for the three-dimensional Laplace operator.

Green's second identity gives for a function ϕ_w harmonic in the test section interior

$$\phi_w(\mathbf{r}_0) = \iint_S \left[\phi_w(\mathbf{r})\frac{\partial G(\mathbf{r}_0, \mathbf{r})}{\partial n} - G(\mathbf{r}_0, \mathbf{r})\frac{\partial \phi_w(\mathbf{r})}{\partial n}\right] dS$$

and for a function ϕ_m harmonic in the test section exterior

$$0 = \iint_S [\phi_m(\mathbf{r}) \frac{\partial G(\mathbf{r}_0,\mathbf{r})}{\partial n} - G(\mathbf{r}_0,\mathbf{r}) \frac{\partial \phi_m(\mathbf{r})}{\partial n}] dS.$$

The differential and integral operations are taken with respect to the unsubscripted coordinates; S is the control surface (interface) enclosing the test section interior, and $\partial/\partial n$ is the derivative along the outward normal to the control surface in the transformed space (x', y, z).

Adding the above formulae and eliminating ϕ_m from Eq.(3), we obtain the correction formula of *Ashill* and *Weeks* [18]:

$$\phi_w(\mathbf{r}_0) = \iint_S [\phi(\mathbf{r}) \frac{\partial G(\mathbf{r}_0,\mathbf{r})}{\partial n} - G(\mathbf{r}_0,\mathbf{r}) \frac{\partial \phi(\mathbf{r})}{\partial n}] dS. \tag{16}$$

It expresses the interior value of the wall interference potential in terms of boundary values of the (total) disturbance velocity potential.

Considering the entire space, Eq.(16) describes a sectionally harmonic function ϕ_w having a jump discontinuity ϕ across the surface S. This differs from the more conventional representation of the wall interference potential by external singularities, where ϕ_w is continuous across S and harmonic everywhere except at the singular points. Of course, inside the test section both representations are equivalent.

Physically, integral (16) can be interpreted as a surface distribution of doublets

$$\frac{\partial G(\mathbf{r}_0,\mathbf{r})}{\partial n} \qquad \text{with density} \qquad \phi(\mathbf{r})$$

and a surface distribution of sources

$$G(\mathbf{r}_0,\mathbf{r}) \qquad \text{with density} \qquad -\frac{\partial \phi(\mathbf{r})}{\partial n}.$$

The normal component of disturbance velocity $\partial\phi/\partial n$ can be measured directly, whereas the potential ϕ has to be evaluated by a streamwise integration of the measured pressure coefficient, Eq.(6).

Another possibility offers the integration by parts [19], converting the surface distribution of doublets into a surface distribution of (horseshoe) vortices

$$\Omega(\mathbf{r}_0,\mathbf{r}) = \int_{x'}^{\infty} \frac{\partial G(\mathbf{r}_0,\mathbf{r})}{\partial n} dx' \qquad \text{with density} \qquad \frac{\partial \phi(\mathbf{r})}{\partial x'} = -\frac{\beta}{2} C_p(\mathbf{r}). \tag{17}$$

The far upstream and downstream terms are eliminated by the virtue of

$$\phi(\mathbf{r}_0,\mathbf{r}) \to 0 \quad \text{as} \quad x' \to -\infty \qquad \text{and} \qquad \Omega(\mathbf{r}_0,\mathbf{r}) \to 0 \quad \text{as} \quad x' \to \infty.$$

Taking in Eq.(16) the limit as $\mathbf{r}_0$ becomes a point of a smooth surface element, we obtain

$$\phi_w(\mathbf{r}_0) = \frac{1}{2}\phi(\mathbf{r}_0) + \iint_S [\phi(\mathbf{r}) \frac{\partial G(\mathbf{r}_0,\mathbf{r})}{\partial n} - G(\mathbf{r}_0,\mathbf{r}) \frac{\partial \phi(\mathbf{r})}{\partial n}] dS, \quad \mathbf{r}_0 \in S. \tag{18}$$

A small circular neighbourhood of the singular point $\mathbf{r}_0$ is to be taken out from the surface S for the doublet integral; its contribution has already been accounted for by the isolated term $\frac{1}{2}\phi(\mathbf{r}_0)$. There is no ambiguity concerning the source integral, as the contribution of a small circular element around the point $\mathbf{r}_0$ is zero.

Another interesting relationship is obtained by substituting Eq.(18) in Eq.(3):

$$\phi_m(\mathbf{r}_0) = \frac{1}{2}\phi(\mathbf{r}_0) - \iint_S [\phi(\mathbf{r})\frac{\partial G(\mathbf{r}_0,\mathbf{r})}{\partial n} - G(\mathbf{r}_0,\mathbf{r})\frac{\partial \phi(\mathbf{r})}{\partial n}]dS, \quad \mathbf{r}_0 \in S. \tag{19}$$

This formula, similar to that developed in Ref.[19], determines the boundary value of the free air potential, ϕ_m, from the measured boundary values of ϕ and $\partial\phi/\partial n$. Provided that the difference between the boundary values of ϕ and ϕ_m is small, it may be possible to achieve $\phi = \phi_m$ in a single adjustment of the walls. Equation (19) will then play the role of a *single-step convergence formula*, a concept introduced in Ref.[20].

Alternative formulations of the correction method based on Green's theorem are given in Refs.[21] and [22], comparisons and accuracy aspects are discussed in Ref.[23]. Model representation, as shown above, is no longer required, but the sparseness of boundary data and incomplete test section boundary remain as a major source of inaccuracy.

The specification of *interference-free conditions* in the two-variable method is straightforward. Setting $\phi_w = 0$ in Eq.(18) or $\phi_m = \phi$ in Eq.(19), we obtain

$$\frac{1}{2}\phi(\mathbf{r}_0) = -\iint_S [\phi(\mathbf{r})\frac{\partial G(\mathbf{r}_0,\mathbf{r})}{\partial n} - G(\mathbf{r}_0,\mathbf{r})\frac{\partial \phi(\mathbf{r})}{\partial n}]dS, \quad \mathbf{r}_0 \in S, \tag{20}$$

which interrelates the values of ϕ and $\partial\phi/\partial n$ on the bounding surface of an adapted test section.

The descent to two dimensions is accomplished by putting

$$\mathbf{r}_0 = (x_0', y_0), \quad \mathbf{r} = (x', y), \quad G(\mathbf{r}_0,\mathbf{r}) = \frac{1}{2\pi}\ln|\mathbf{r}_0 - \mathbf{r}|,$$

and replacing the surface integrals by contour integrals.

However, more readily applicable results are obtained using Cauchy's integral formula. To illustrate this approach, we introduce the complex coordinate

$$z = x' + iy = \frac{x}{\beta} + iy \tag{21}$$

and the complex disturbance velocity

$$w(z) = \beta u(x,y) - iv(x,y) = \beta\frac{\partial\phi}{\partial x}(x,y) - i\frac{\partial\phi}{\partial y}(x,y). \tag{22}$$

In accordance with Eq.(3), the complex disturbance velocity is decomposed as

$$w(z) = w_m(z) + w_w(z), \tag{23}$$

where w_w is analytic in the test section interior and w_m is analytic in the test section exterior. Applying the Cauchy integral formula to a counterclockwise oriented contour C, we obtain for an interior point z_0

$$w_w(z_0) = \frac{1}{2\pi i}\int_C \frac{w_w(z)}{z - z_0}dz$$

and

$$0 = \frac{1}{2\pi i}\int_C \frac{w_m(z)}{z - z_0}dz.$$

Adding the integrals and eliminating w_m from Eq.(23), we obtain *Smith's* correction formula [4]:

$$w_w(z_0) = \frac{1}{2\pi i}\int_C \frac{w(z)}{z - z_0}dz, \tag{24}$$

expressing the wall interference velocity in terms of boundary value of the (total) disturbance velocity.

The Cauchy type integral along a curved path can be evaluated as indicated in Appendix. Using Eq.(22), the components of the wall interference velocity are obtained as:

$$u_w(x_0, y_0) = \frac{1}{\beta}\mathrm{Re}\{w_w(z_0)\} \qquad \text{and} \qquad v_w(x_0, y_0) = -\mathrm{Im}\{w_w(z_0)\}. \tag{25}$$

An example of wall deflections and wall pressures from the tests [24] of the 9-in chord CAST 10-2/DOA 2 airfoil in the 13-in by 13-in flexible-wall test section of the Langley Transonic Cryogenic Wind Tunnel (TCT) is shown in Fig.2. The wall pressure distribution at the stream Mach number of 0.7 is subcritical as required. The downstream end of the integration contour was placed so as to cut off the last three pressure points, drifting away from the undisturbed flow conditions. The distribution of residual corrections along the wind tunnel axis, evaluated by the two-variable method, is shown in Fig.3. The flow in the test section is not interference free, but considering the size of the model with respect to the test section, the corrections are certainly small.

More detailed formulae, together with residual interference evaluated for the ONERA/CERT T2 flexible wall wind tunnel, can be found in Ref.[25].

Considering the entire complex plane, Eq.(24) describes a sectionally analytic function w_w having a jump discontinuity w across the contour C. This is obviously in contrast with the conventional representation of the complex interference velocity by external poles, allowing w_w to be analytically continued across C, but only up to the location of the poles.

The Cauchy-type integral (24) can be recast into the contour integral

$$w_w(z_0) = \int_C \left[\frac{i\gamma(z)}{2\pi(z_0 - z)} + \frac{\sigma(z)}{2\pi(z_0 - z)}\right]ds, \tag{26}$$

where $ds = |dz|$ is the counterclockwise oriented contour length element.

The integral can be interpreted as a line distribution of vortices

$$\frac{i}{2\pi(z_0 - z)} \qquad \text{with density} \qquad \gamma(z) = \mathrm{Re}\left\{ w(z)\frac{dz}{|dz|} \right\} = q_t(z) \tag{27}$$

and a line distribution of sources

$$\frac{1}{2\pi(z_0 - z)} \qquad \text{with density} \qquad \sigma(z) = -\mathrm{Im}\left\{ w(z)\frac{dz}{|dz|} \right\} = -q_n(z), \tag{28}$$

where q_t is the tangent component of disturbance velocity (positive in the counterclockwise direction) and q_n is the normal component of disturbance velocity (positive in the direction of the outward normal). The correspondence with Green's theorem approach is evident.

The *autocorrective property* of Eq.(24) again applies [15] and is easy to verify. Starting with the reference velocity increment δU_∞, the boundary value of the x-component of disturbance velocity

$$u = \frac{U - U_\infty}{U_\infty}$$

is found to have an increment

$$\delta u = \frac{U - (U_\infty + \delta U_\infty)}{U_\infty + \delta U_\infty} - u \simeq -\frac{\delta U_\infty}{U_\infty}.$$

From Eqs.(22) and (24) it follows for the increment of the complex disturbance velocity at an interior point z_0

$$\delta w_w(z_0) = \frac{\beta\,\delta u}{2\pi i}\int_C \frac{dz}{z - z_0} = \beta\,\delta u.$$

Finally, from Eqs.(25)

$$\delta u_w(x_0, y_0) = \delta u \simeq -\frac{\delta U_\infty}{U_\infty},$$

$$\delta v_w(x_0, y_0) = 0.$$

A practical verification of the autocorrective property is shown in Fig.4. The reference Mach number of our example in Fig.2 was tentatively changed from 0.700 to 0.695 and the wall pressure coefficients, used as input for the residual interference calculation, were recalculated accordingly. Comparing Fig.4 with Fig.3, we note that the resultant Mach number correction curve is displaced by 0.005 in the positive direction, so that the corrected Mach number is again the same. The angle of attack correction, as expected, is not greatly affected by the change of the reference Mach number.

Correction formula (24) is closely related to wall adaptation criteria for two-dimensional testing. In the limiting process, as z_0 becomes a point on a smooth segment of the contour C we obtain

$$w_w(z_0) = \frac{1}{2}w(z_0) + \frac{1}{2\pi i}\int_C \frac{w(z)}{z - z_0}dz, \quad z_0 \in C, \tag{29}$$

where the (singular) integral is to be interpreted as Cauchy's principal value.

Substituting Eq.(29) in (23), we find

$$w_m(z_0) = \frac{1}{2}w(z_0) - \frac{1}{2\pi i}\int_C \frac{w(z)}{z - z_0}dz, \quad z_0 \in C, \tag{30}$$

which is the limiting case of the formula given in Ref.[26]. It determines the boundary value w_m of the complex disturbance velocity due to the model in free air, in terms of the measured values w. This result proves again that the model representation in the two-variable method is, in theory, superfluous. However, for incomplete boundary data an independently estimated far field of w_m may conveniently be used to aid the interpolations and extrapolations.

Equation (30) may also be used as the two-dimensional *single-step convergence formula*; the case of straight line boundaries can be found in Refs.[20] and [27].

Setting $w_w = 0$ in Eq.(29) or $w_m = w$ in Eq.(30), we obtain the *interference-free condition*

$$\frac{1}{2}w(z_0) = -\frac{1}{2\pi i}\int_C \frac{w(z)}{z - z_0}dz, \quad z_0 \in C \tag{31}$$

in terms of the complex disturbance velocity on the boundary. The factor $\frac{1}{2}$ was left uncancelled, to emphasize the connection with the three-dimensional condition, Eq.(20).

Considering straight line boundaries at $y = \pm\frac{h}{2}$, we obtain in terms of disturbance velocity components

$$u(x_0, \pm\frac{h}{2}) = \mp\frac{1}{\beta\pi}\int_{-\infty}^{\infty} \frac{v(x, \pm\frac{h}{2})}{x - x_0}dx, \tag{32a}$$

$$v(x_0, \pm\frac{h}{2}) = \pm\frac{\beta}{\pi}\int_{-\infty}^{\infty} \frac{u(x, \pm\frac{h}{2})}{x - x_0}dx. \tag{32b}$$

These 'compressible-flow' versions of Hilbert's transforms, introduced by *Sears* [1] as *functional relationships* between two velocity components, define unconfined flow in a two-dimensional test section.

C. Interface Discontinuity Method

This residual interference method, closely related to the two-variable method, utilizes exterior flow calculations. The general idea, as proposed by *Sears* and *Erickson* [28] is essentially this: the flow field is considered to consist of an experimental inner region joined at an interface to a computed outer region. If the computed outer flow satisfies the unconfined flow conditions and matches along the interface the inner flow, then the combined flow field is continuous, representing unconfined flow around the model. The matching error, or discontinuity, provides a measure of the residual interference. It can be quantified by removing the discontinuity by a surface distribution of singularities. These singularities do not disturb the unconfined flow condition in the outer region, but do introduce velocity perturbations at the position of the test model, which then can be interpreted as the usual wall interference corrections.

As for the two-component method, Green's theorem will give us a quick answer as to what the suitable singularities and their densities should be. Selecting $\mathbf{r}_0$ to be an interior point, we obtain for the function $\widetilde{\phi}$, representing the disturbance velocity potential of the fictitious flow in the exterior region

$$0 = \iint_S [\widetilde{\phi}(\mathbf{r}) \frac{\partial G(\mathbf{r}_0, \mathbf{r})}{\partial n} - G(\mathbf{r}_0, \mathbf{r}) \frac{\partial \widetilde{\phi}(\mathbf{r})}{\partial n}] dS.$$

Subtracting it from Eq.(16), we obtain the interior value of the wall interference potential in terms of the differences of the interior and exterior flow potentials and their normal derivatives along the interface:

$$\phi_w(\mathbf{r}_0) = \iint_S \left\{ [\phi(\mathbf{r}) - \widetilde{\phi}(\mathbf{r})] \frac{\partial G(\mathbf{r}_0, \mathbf{r})}{\partial n} - [\frac{\partial \phi(\mathbf{r})}{\partial n} - \frac{\partial \widetilde{\phi}(\mathbf{r})}{\partial n}] G(\mathbf{r}_0, \mathbf{r}) \right\} dS. \tag{33}$$

Physically, integral (33) can be interpreted as a surface distribution of doublets

$$\frac{\partial G(\mathbf{r}_0, \mathbf{r})}{\partial n} \qquad \text{with density} \qquad [\phi(\mathbf{r}) - \widetilde{\phi}(\mathbf{r})]$$

and a surface distribution of sources

$$G(\mathbf{r}_0, \mathbf{r}) \qquad \text{with density} \qquad - [\frac{\partial \phi(\mathbf{r})}{\partial n} - \frac{\partial \widetilde{\phi}(\mathbf{r})}{\partial n}].$$

The potential $\widetilde{\phi}$ is obtained by solving an exterior flow problem (CFD), but ϕ_w is obtained by a surface integration, as in the two-variable method.

The exterior flow can be calculated as a solution of a Neumann problem, satisfying the boundary condition

$$\frac{\partial \widetilde{\phi}(\mathbf{r})}{\partial n} = \frac{\partial \phi(\mathbf{r})}{\partial n}, \quad \mathbf{r} \in S, \tag{34}$$

where $\partial \phi(\mathbf{r})/\partial n$ is the normal component of disturbance velocity on the interface. Integral (33) then reduces to the distribution of doublets,

$$\phi_w(\mathbf{r}_0) = \iint_S [\phi(\mathbf{r}) - \widetilde{\phi}(\mathbf{r})] \frac{\partial G(\mathbf{r}_0, \mathbf{r})}{\partial n} dS. \tag{35}$$

Alternatively, the exterior flow can be calculated as a solution of a Dirichlet problem, satisfying the boundary condition

$$\widetilde{\phi}(\mathbf{r}) = \phi(\mathbf{r}), \quad \mathbf{r} \in S, \tag{36}$$

integral (33) reduces to the distribution of sources,

$$\phi_w(\mathbf{r}_0) = - \iint_S [\frac{\partial \phi(\mathbf{r})}{\partial n} - \frac{\partial \widetilde{\phi}(\mathbf{r})}{\partial n}] G(\mathbf{r}_0, \mathbf{r}) dS. \tag{37}$$

The latter approach has recently been described by *Rebstock* and *Lee* [29].

Finally, if the walls are adjusted to satisfy the conditions (34) and (36) simultaneously (a perfect match), then from Eq.(33)

$$\phi_w(r_0) \equiv 0,$$

indicating that the flow inside the test section is interference free. The conditions of flow tangency and equal pressures along the interface imply that the desired interface is a stream tube. This streamlining principle for an adaptive wall test section, introduced by *Goodyer* [2], is of course quite general and not just restricted to linear subsonic flow.

The Cauchy integral approach, applicable to two-dimensional flow, proceeds along the similar lines. Considering the complex disturbance velocity $\tilde{w}$ of the fictitious flow, analytic in the exterior region and vanishing at infinity, then for an interior point z_0 it follows

$$0 = \frac{1}{2\pi i}\int_C \frac{\tilde{w}(z)}{z - z_0}dz.$$

Subtracting it from Eq.(24), we obtain

$$w_w(z_0) = \frac{1}{2\pi i}\int_C \frac{w(z) - \tilde{w}(z)}{z - z_0}dz. \tag{38}$$

This Cauchy type integral can again be evaluated as described in Appendix.

If the normal component of disturbance velocity is continuous across the interface,

$$\tilde{q}_n(z) = q_n(z), \quad z \in C, \tag{39}$$

then from Eqs.(27)-(28)

$$w_w(z_0) = \int_C \left[(q_t(z) - \tilde{q}_t(z)\right] \frac{i}{2\pi(z_0 - z)}ds. \tag{40}$$

The wall interference velocity is represented by contour distribution vortices, whose density is equal to the discontinuity of the tangential component of velocity.

Conversely, if the tangential component of disturbance velocity is continuous,

$$\tilde{q}_t(z) = q_t(z), \quad z \in C, \tag{41}$$

then

$$w_w(z_0) = \int_C -\left[(q_n(z) - \tilde{q}_n(z)\right] \frac{1}{2\pi(z_0 - z)}ds. \tag{42}$$

The wall interference velocity is represented by contour distribution sources, whose density is equal and opposite to the discontinuity of the normal component of velocity.

The single-step convergence formula of *Judd, Wolf,* and *Goodyer* [30] can be derived from Eq.(38) by taking the limit as as z_0 becomes a point of interface C, by analogy with Eqs.(24) and (29), and eliminating w_w from Eq.(23).

Appendix

The Cauchy type integral, Eq.(24) or (38), is easily evaluated by using a technique from Ref.[31]. Approximating the contour C by line segments, the integral

$$w_w(z_0) = \frac{1}{2\pi i}\int_C \frac{f(z)}{z - z_0}dz \tag{43}$$

reduces to the sum

$$w_w(z_0) = \sum_j \Delta_j w_w(z_0), \tag{44}$$

where

$$\Delta_j w_w(z_0) = \frac{1}{2\pi i}\int_{z_j}^{z_{j+1}} \frac{f(z)}{z - z_0}dz \tag{45}$$

is the contribution of the j-th segment.

Assuming a linear variation of the density function f between the segment end points z_j and z_{j+1}:

$$\begin{aligned} f(z) &= f_j + \frac{f_{j+1} - f_j}{z_{j+1} - z_j}(z - z_j) \\ &= \frac{f_{j+1} - f_j}{z_{j+1} - z_j}(z - z_0) + f_{j+1}\frac{z_0 - z_j}{z_{j+1} - z_j} - f_j\frac{z_0 - z_{j+1}}{z_{j+1} - z_j} \end{aligned} \tag{46}$$

and substituting it in Eq.(45), we find

$$\Delta_j w_w(z_0) = \frac{f_{j+1} - f_j}{2\pi i} + \frac{1}{2\pi i}\left[f_{j+1}\frac{z_0 - z_j}{z_{j+1} - z_j} - f_j\frac{z_0 - z_{j+1}}{z_{j+1} - z_j}\right]\ln\frac{z_{j+1} - z_0}{z_j - z_0}. \tag{47}$$

References

[1] Sears, W.R., "Self Correcting Wind Tunnels," The Aeronautical Journal, Vol.78, March 1974, pp.80-89.

[2] Goodyer, M.J., "The Self Streamlining Wind Tunnel," NASA TMX-72699, Aug.1975.

[3] Kraft, E.M., Ritter, A., and Laster, M.L., "Advances at AEDC in Treating Transonic Wind Tunnel Wall Interference," ICAS Proceedings 1986, pp.748-769.

[4] Smith, J., "Measured Boundary Conditions for 2D Flow," AGARD-CP-335, May 1982, pp.9.1 - 9.15.

[5] Baldwin,B.S., Turner, J.B., and Knechtel, E.D., "Wall Interference in Wind Tunnels With Slotted and Porous Boundaries at Subsonic Speeds," NACA TN 3176, 1954.

[6] Garner, H.C., Rogers, E.W.E., Acum, W.E.A., and Maskell, E.C.,"Subsonic Wind Tunnel Wall Corrections," AGARDograph 109, Oct.1966.

[7] Capelier, C., Chevallier, J.P., and Bouniol, F., "Nouvelle méthode de correction des effets de parois en courant plan," La recherche aérospatiale, Jan.-Feb. 1978, pp.1-11.

[8] Stakgold, I., *Boundary Value Problems of Mathematical Physics*, Vol.II, Macmillan, 1968.

[9] Mokry, M., Digney, J.R., and Poole, R.J.D., "Doublet-Panel Method for Half-Model Wind-Tunnel Corrections," Journal of Aircraft, Vol.24, May 1987, pp.322-327.

[10] Mokry, M. and Ohman, L.H., "Application of the Fast Fourier Transform to Two-Dimensional Wind Tunnel Wall Interference," Journal of Aircraft, Vol.17, June 1980, pp.402-408.

[11] Mokry, M., "Subsonic Wall Interference Corrections for Finite-Length Test Sections Using Boundary Pressure Measurements," AGARD-CP-335, May 1982, pp.10.1 - 10.15.

[12] Rizk, M.H. and Smithmeyer, M.G., "Wind-Tunnel Interference Corrections for Three-Dimensional Flows," Journal of Aircraft, Vol.19, June 1982, pp.465-472.

[13] Gakhov, F.D., *Boundary Value Problems*, Pergamon Press, 1966.

[14] Chevallier, J.P., "Survey of ONERA Activities on Adaptive-Wall Applications and Computation of Residual Corrections," Wind Tunnel Wall Interference Assessment/Correction 1983, NASA CP 2319, 1984, pp.43-58.

[15] GARTEUR Action Group AD(AG-23), "Two-Dimensional Transonic Testing Methods," NLR TR 83086 U, July 1981.

[16] Archambaud, J.P. and Chevallier, J.P., "Utilisation de parois adaptables pour les essais en courant plan," AGARD-CP-335, May 1982, pp.14.1 - 14.14.

[17] Paquet, J.B., "Perturbations induites par les parois d'une soufflerie - methods intégrales," Thèse Ing. Doc., Université de Lille, 1979.

[18] Ashill, P.R. and Weeks, D.J., "A Method for Determining Wall-Interference Corrections in Solid-Wall Tunnels from Measurements of Static Pressure at the Walls," AGARD-CP-335, May 1982, pp.1.1 - 1.12.

[19] Ashill, P.R. and Keating, R.F.A., "Calculation of Tunnel Wall Interference from Wall-Pressure Measurements," Journal of the Royal Aeronaut. Soc., Jan.1988, pp.36-53.

[20] Lo, C.F. and Kraft, E.M., "Convergence of the Adaptive-Wall Wind Tunnel," AIAA Journal, Vol.16, Jan.1978, pp.67-72.

[21] Barche, J., "Zur Ermittlung von Wandinterferenzen," Zeitschrift für Flugwiss. und Weltraumforschung, 4, 1980, pp.389-396.

[22] Labrujère Th.E., "Correction for Wall-Interference by Means of a Measured-Boundary-Condition Method", NLR TR 84114 U, Nov.1984.

[23] Maarsingh, R.A., Labrujère Th.E., and Smith, J., "Accuracy of Various Wall-Correction Methods for 3D Subsonic Wind Tunnel Testing," AGARD-CP-429, Sept.1987, pp.17.1 - 17.13.

[24] Mineck, R.E., "Wall Interference Tests of a CAST 10-2/DOA 2 Airfoil in an Adaptive-Wall Test Section," Supplement to NASA TM 4015, Dec.1987.

[25] Amecke, J., "Direkte Berechnung von Wandinterferenzen und Wandadaptation bei zweidimensionaler Strömung in Windkanälen mit geschlossenen Wänden," DFVLR-FB 85-62, Nov.1985; also NASA TM-88523, Dec.1986.

[26] Niederdrenk, P. and Wedemeyer, E., "Analytic Near-Field Boundary Condition for Transonic Flow Computations," AIAA Journal, Vol.25, June 1987, pp.884 - 886.

[27] Kraft, E.M. and Dahm, W.J.A., "Direct Assessment of Wall Interference in a Two-Dimensional Subsonic Wind Tunnel," AIAA-82-0187, Jan.1982.

[28] Sears, W.R. and Erickson, J.C.Jr., "Adaptive Wind Tunnels," Ann.Rev.Fluid Mech., Vol.20, 1988, pp.17-34.

[29] Rebstock, R., and Lee E.E.Jr., "Capabilities of Wind Tunnels With Two Adaptive Walls to Minimize Boundary Interference in 3-D Model Testing," Transonic Symposium, NASA Langley, April 1988.

[30] Judd, M., Wolf, S.W.D., and Goodyer, M.J., "Analytical Work in Support of the Design and Operation of Two Dimensional Self Streamlining Test Sections," NASA CR 148196, March 1976.

[31] Hromadka II, T.V., *The Complex Variable Boundary Element Method*, Springer-Verlag, 1984.

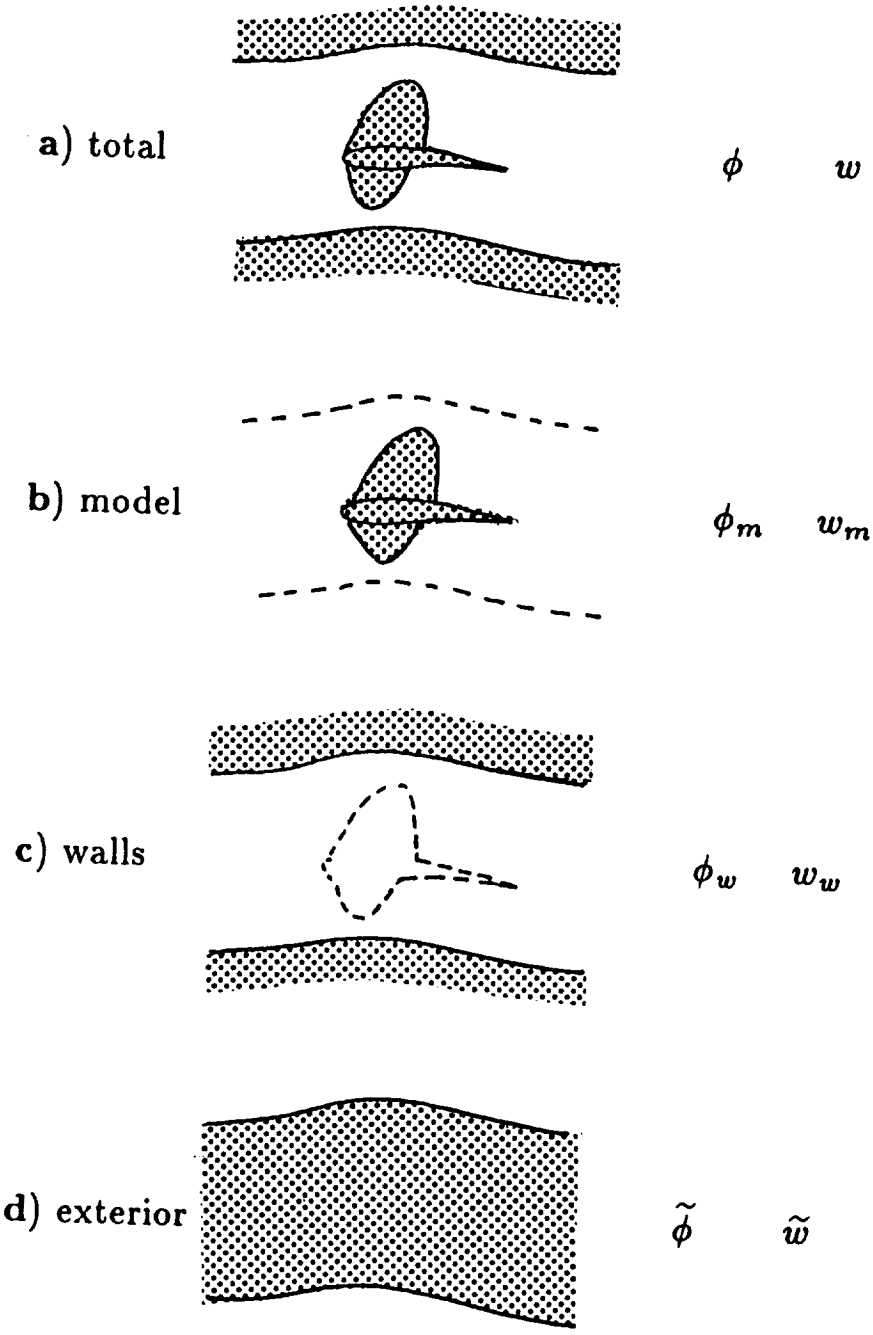

Fig. 1 Linearized flow regions.

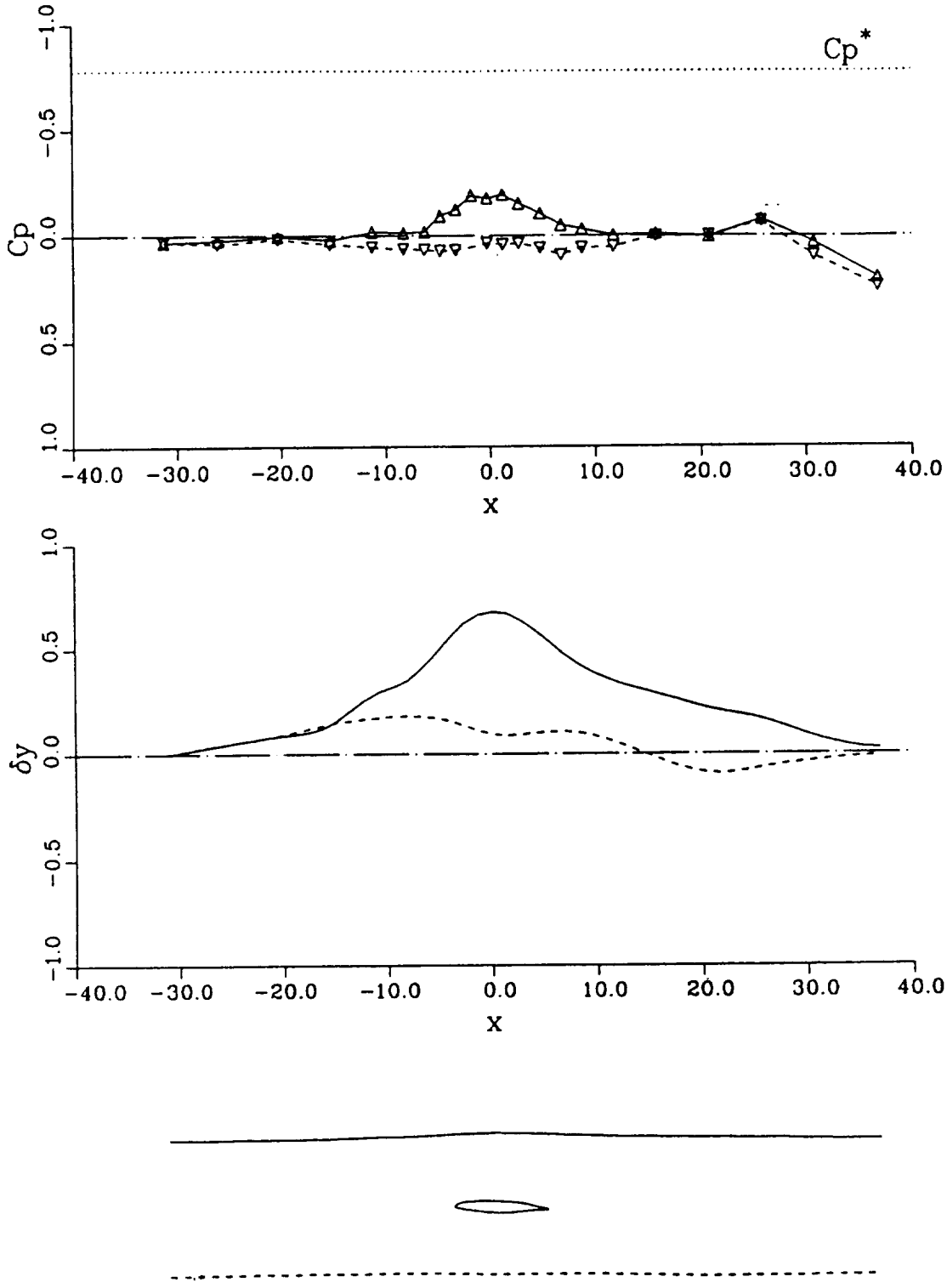

Fig. 2 Wall deflections and wall pressure coefficients; 9-in chord CAST 10 airfoil in the 13-in × 13-in test section of NASA TCT, $M_\infty = 0.700$, $\alpha = 1.20^o$, $C_N = 0.50$.

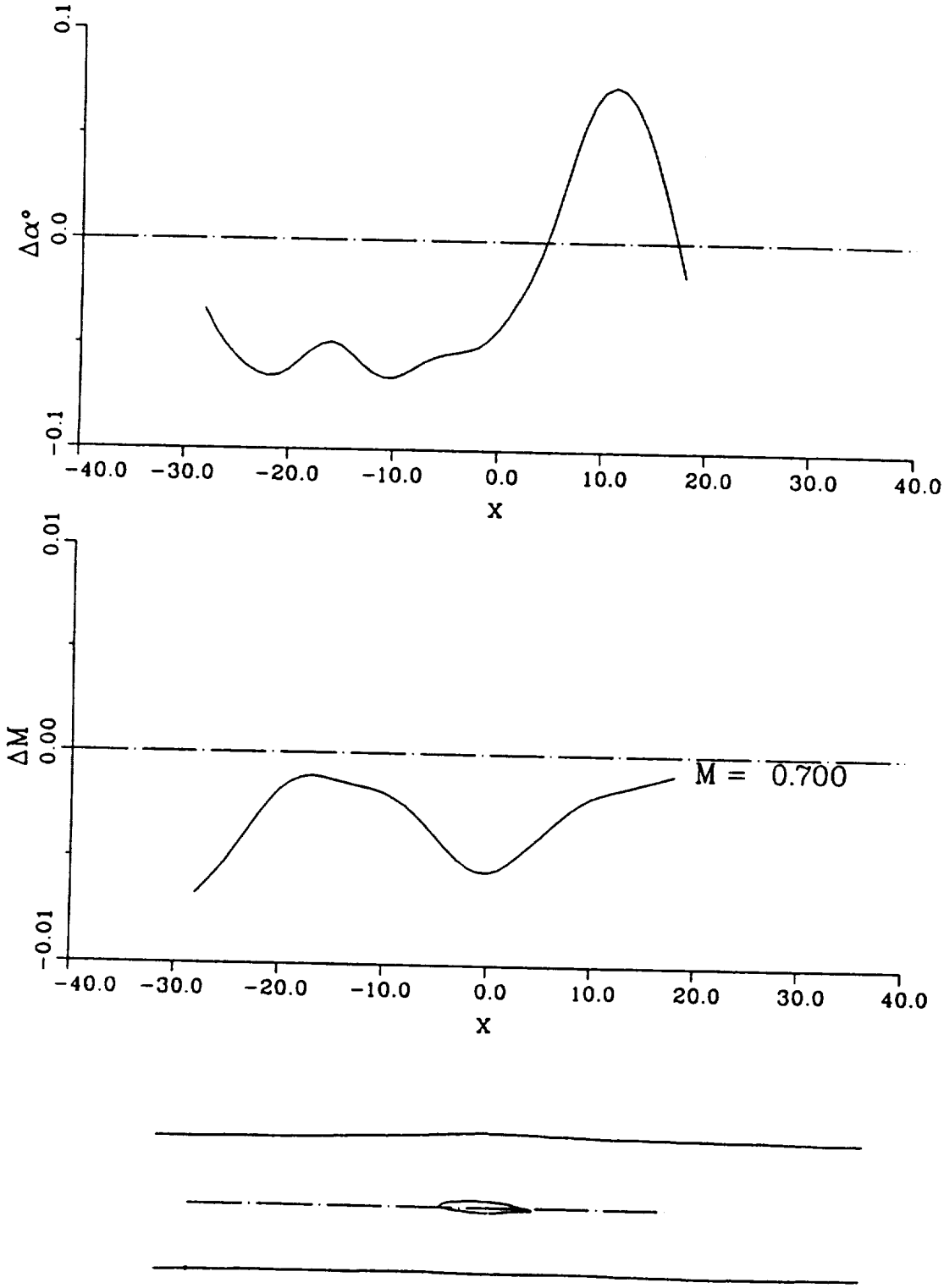

Fig. 3 Residual corrections along test section axis, evaluated by two-variable method from data of Fig.2, $M_\infty = 0.700$.

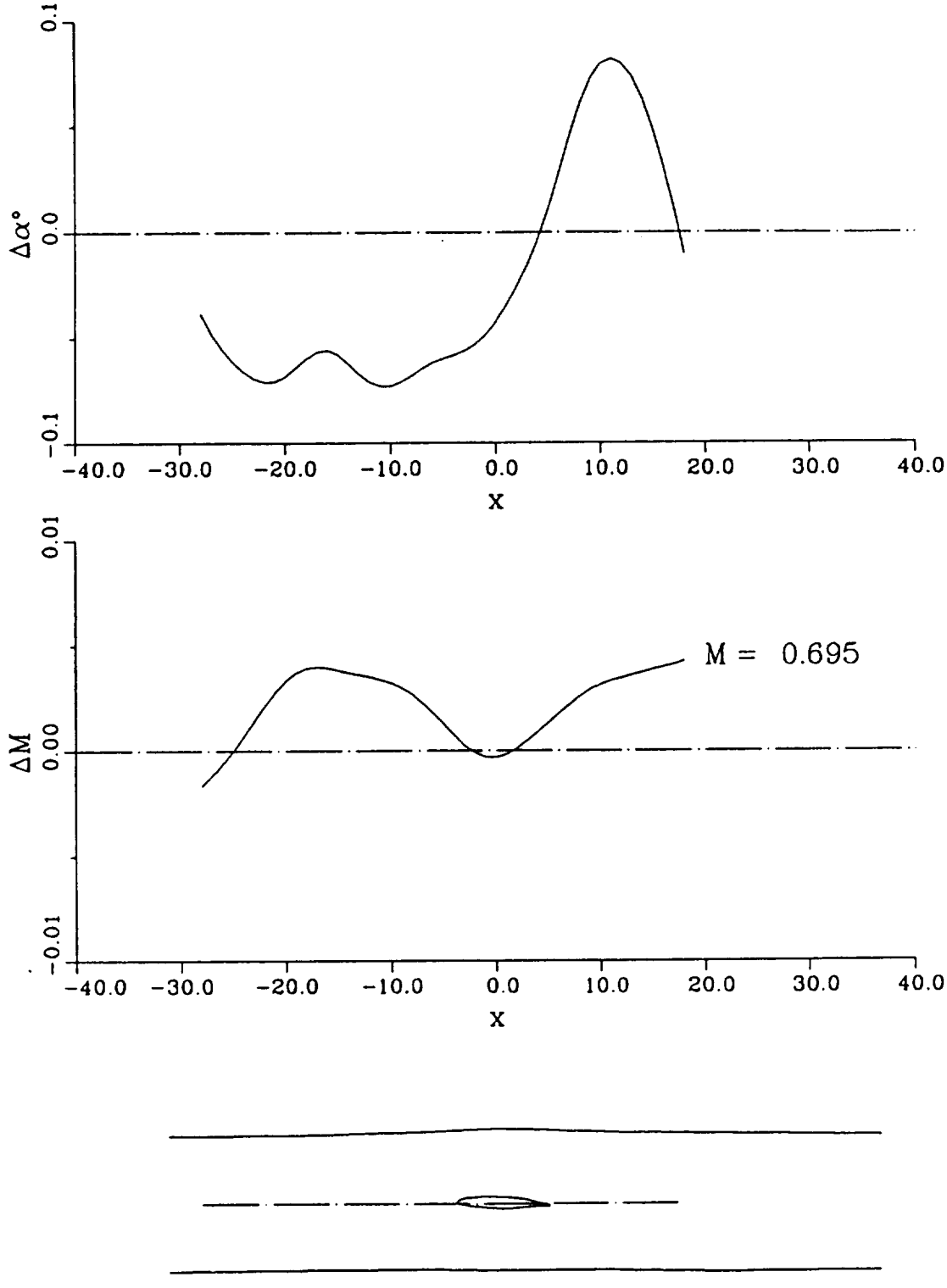

Fig. 4 Residual corrections along test section axis, evaluated by two-variable method from data of Fig.2, setting $M_\infty = 0.695$.